

AFB-0053-FM-9740-841

AEOSR-IR 94 0623

**AD-A285 872**



**NOVEL E-O POLYMERS: NLO MATERIALS WITH SUPERIOR TEMPORAL STABILITY**

M. Druy  
Foster-Miller, Inc.  
350 Second Avenue  
Waltham, MA 02154-1196

September 1994

Final Technical Report  
Contract No. F49620-93-C-0053

DTIC  
ELECTE  
NOV 01 1994  
S G D

DTIC QUALITY INSPECTED 2

Prepared for

United States Air Force  
Air Force Materiel Command  
Air Force Office of Scientific Research  
110 Duncan Avenue  
Bolling AFB, DC 20332-0001



9 4 - 0 0 0 0

2419 94-33829



142400

AFB-0053-FM-9740-841

**NOVEL E-O POLYMERS: NLO MATERIALS WITH SUPERIOR  
TEMPORAL STABILITY**

M. Druy  
Foster-Miller, Inc.  
350 Second Avenue  
Waltham, MA 02154-1196

September 1994

Final Technical Report  
Contract No. F49620-93-C-0053

Accession For	
NTIS CRA&I	<input checked="" type="checkbox"/>
DTIC TAB	<input checked="" type="checkbox"/>
Unannounced	<input type="checkbox"/>
Justification .....	
By .....	
Distribution /	
Availability Codes	
Dist	Avail and/or Special
A-1	

Prepared for

United States Air Force  
Air Force Materiel Command  
Air Force Office of Scientific Research  
110 Duncan Avenue  
Bolling AFB, DC 20332-0001

**LICENSE RIGHTS LEGEND**  
Contract No. F49620-93-C-0053  
Contractor or Subcontractor: Foster-Miller, Inc.

*For a period of four (4) years after the delivery and acceptance of the last deliverable item under the above contract, this technical data shall be subject to the restrictions contained in the definition of "Limited Rights" in DFARS clause at 252.227-7013. After the four-year period, the data shall be subject to the restrictions contained in the definition of "Government Purpose License Rights" in DFARS clause 252.227-7013. The Government assumes no liability for unauthorized use or disclosure by others. This legend, together with the indications of the portions of the data which are subject to such limitations shall be included on any reproduction hereof which contains any portions subject to such limitations and shall be honored only as long as the data continues to meet the definition on Government purpose license rights.*



OFFICE OF THE UNDER SECRETARY OF DEFENSE (ACQUISITION)  
DEFENSE TECHNICAL INFORMATION CENTER  
CAMERON STATION  
ALEXANDRIA, VIRGINIA 22304-6145

Oct 13, 1994

IN REPLY  
REFER TO

DTIC-OCC

SUBJECT: Distribution Statements on Technical Documents

TO:

AFOSR/XPT  
Bolling AFB, DC 20332-0001

1. Reference: DoD Directive 5230.24, Distribution Statements on Technical Documents, 18 Mar 87.

2. The Defense Technical Information Center received the enclosed report (referenced below) which is not marked in accordance with the above reference.

Final Technical report  
Sep 94  
F49620-93-C-0053

3. We request the appropriate distribution statement be assigned and the report returned to DTIC within 5 working days.

4. Approved distribution statements are listed on the reverse of this letter. If you have any questions regarding these statements, call DTIC's Cataloging Branch, (703) 274-6837.

FOR THE ADMINISTRATOR:

1 Encl

GOPALAKRISHNAN NAIR  
Chief, Cataloging Branch

*AFOSR/XPT*  
*Recvd*  
*10/18/94*  
*sent Back*  
*10/18/94*

FL-171  
Jul 93

**DISTRIBUTION STATEMENT A:**

**APPROVED FOR PUBLIC RELEASE: DISTRIBUTION IS UNLIMITED**

**DISTRIBUTION STATEMENT B:**

**DISTRIBUTION AUTHORIZED TO U.S. GOVERNMENT AGENCIES ONLY;**  
(Indicate Reason and Date Below). OTHER REQUESTS FOR THIS DOCUMENT SHALL BE REFERRED  
TO (Indicate Controlling DoD Office Below).

**DISTRIBUTION STATEMENT C:**

**DISTRIBUTION AUTHORIZED TO U.S. GOVERNMENT AGENCIES AND THEIR CONTRACTORS;**  
(Indicate Reason and Date Below). OTHER REQUESTS FOR THIS DOCUMENT SHALL BE REFERRED  
TO (Indicate Controlling DoD Office Below).

**DISTRIBUTION STATEMENT D:**

**DISTRIBUTION AUTHORIZED TO DOD AND U.S. DOD CONTRACTORS ONLY;** (Indicate Reason  
and Date Below). OTHER REQUESTS SHALL BE REFERRED TO (Indicate Controlling DoD Office Below).

**DISTRIBUTION STATEMENT E:**

**DISTRIBUTION AUTHORIZED TO DOD COMPONENTS ONLY;** (Indicate Reason and Date Below).  
OTHER REQUESTS SHALL BE REFERRED TO (Indicate Controlling DoD Office Below).

**DISTRIBUTION STATEMENT F:**

**FURTHER DISSEMINATION ONLY AS DIRECTED BY** (Indicate Controlling DoD Office and Date  
Below) **or HIGHER DOD AUTHORITY.**

**DISTRIBUTION STATEMENT X:**

**DISTRIBUTION AUTHORIZED TO U.S. GOVERNMENT AGENCIES AND PRIVATE INDIVIDUALS  
OR ENTERPRISES ELIGIBLE TO OBTAIN EXPORT-CONTROLLED TECHNICAL DATA IN ACCORDANCE  
WITH DOD DIRECTIVE 5230.25, WITHHOLDING OF UNCLASSIFIED TECHNICAL DATA FROM PUBLIC  
DISCLOSURE, 6 Nov 1984 (Indicate date of determination). CONTROLLING DOD OFFICE IS (Indicate  
Controlling DoD Office).**

The cited documents has been reviewed by competent authority and the following distribution statement is  
hereby authorized.

\_\_\_\_\_  
(Statement)

\_\_\_\_\_  
(Controlling DoD Office Name)

\_\_\_\_\_  
(Reason)

\_\_\_\_\_  
(Controlling DoD Office Address,  
City, State, Zip)

\_\_\_\_\_  
(Signature & Typed Name)

\_\_\_\_\_  
(Assigning Office)

\_\_\_\_\_  
(Date Statement Assigned)

Dist: A

# REPORT DOCUMENTATION PAGE

Form Approved  
OMB No. 0704-0188

Public reporting burden for this collection of information is estimated to average 1 hour per response, including the time for reviewing instructions, searching existing data sources, gathering and maintaining the data needed, and completing and reviewing the collection of information. Send comments regarding this burden estimate or any other aspect of this collection of information, including suggestions for reducing this burden, to Washington Headquarters Services, Directorate for Information Operations and Reports, 1215 Jefferson Davis Highway, Suite 1204, Arlington, VA 22202-4302, and to the Office of Management and Budget, Paperwork Reduction Project (0704-0188), Washington, DC 20503

1. AGENCY USE ONLY (Leave blank)	2. REPORT DATE September 1994	3. REPORT TYPE AND DATES COVERED Final Technical Report July 1993 to July 1994
----------------------------------	----------------------------------	--

4. TITLE AND SUBTITLE Novel E-O Polymers: NLO Materials with Superior Temporal Stability	5. FUNDING NUMBERS FQ8671-9301313 3005/SS
---	--

6. AUTHOR(S) M. Druy
-------------------------

7. PERFORMING ORGANIZATION NAME(S) AND ADDRESS(ES)  Foster-Miller, Inc. 350 Second Avenue Waltham, MA 02154-1196	8. PERFORMING ORGANIZATION REPORT NUMBER  NAS-3988-FM-94101-839 <b>AEOSR-TR- 94 0626</b>
--	---

9. SPONSORING/MONITORING AGENCY NAME(S) AND ADDRESS(ES) United States Air Force; Air Force Materiel Command; Air Force Office of Scientific Research; 110 Duncan Avenue; Bolling AFB, DC 20332-0001	10. SPONSORING/MONITORING AGENCY REPORT NUMBER  F49620-93-C-0053
--	--

11. SUPPLEMENTARY NOTES Administrative Contracting Officer; AFOSR/PKA; 110 Duncan Avenue; Suite B115; Bolling AFB, DC 20332-0001
---

12a. DISTRIBUTION/AVAILABILITY STATEMENT Rights to this data shall be in accordance with Clause 52.227-20, Rights in Data - SBIR Program	12b. DISTRIBUTION CODE <b>A</b> N/A
---	--

13. ABSTRACT (Maximum 200 words)  This report contains experimental results on a comprehensive study of the second order nonlinear optical (NLO) properties of a molecularly doped polymer system. A second-order NLO chromophore, 4-morpholino-4-nitrostilbene (MNS) was synthesized which possesses a large molecular first hyperpolarizability and dipole moment. The chromophore was doped into a polymer matrix with a high glass transition temperature and subsequently poled by a strong electric field to induce noncentrosymmetry required for second-order nonlinear optical behavior. An in situ poling technique was employed to determine the processing and poling parameters in order to obtain high and stable nonlinearities. Detailed information on the synthesis, processing, characterization, and results on a series of samples is presented.
---

14. SUBJECT TERM Materials, second order nonlinear optical materials, nonlinear optics	15. NUMBER OF PAGES 25
	16. PRICE CODE N/A

17. SECURITY CLASSIFICATION OF REPORT Unclassified	18. SECURITY CLASSIFICATION OF THIS PAGE Unclassified	19. SECURITY CLASSIFICATION OF ABSTRACT Unclassified	20. LIMITATION OF ABSTRACT Unlimited
---	--	---	---

# CONTENTS

---

<b>Section</b>		<b>Page</b>
<b>1.</b>	<b>INTRODUCTION</b> .....	<b>1</b>
1.1	Low Temperature Processing - Key to Stability .....	2
1.2	Summary of Phase I Research .....	2
<b>2.</b>	<b>BACKGROUND</b> .....	<b>3</b>
2.1	Electro-Optical and Second Harmonic Generation Waveguide Device Requirements ...	3
2.2	Novel, Room Temperature Processible, Stable Electro-Optic Polymers .....	6
2.3	Principle of Poling Induced Second-Order Nonlinearity in NLO Films .....	7
<b>3.</b>	<b>EXPERIMENTAL PROCEDURES</b> .....	<b>10</b>
3.1	Materials and Sample Preparation .....	10
3.2	Setup for SHG Measurements .....	10
<b>4.</b>	<b>RESULTS AND DISCUSSION</b> .....	<b>13</b>
4.1	Poling Characteristics of Tested Film Samples .....	13
4.2	SHG Decay Behavior of Poled Film Samples .....	16
<b>5.</b>	<b>CONCLUSIONS</b> .....	<b>18</b>
<b>6.</b>	<b>REFERENCES</b> .....	<b>19</b>

## ILLUSTRATIONS

---

Figure		Page
1.	Structure of polyarylate .....	2
2.	Structure of NLO chromophore, MNS .....	2
3.	Mach-Zehnder interferometer .....	3
4.	The difference between the optical and microwave velocities limits the ultimate bandwidth of a traveling wave modulator .....	5
5.	Angular dependence of the SHG intensity from an electric field poled thin film for different polarization combinations.....	9
6.	Mass spectroscopy (upper trace) and <sup>1</sup> H-NMR (bottom trace) spectra of MNS chromophore .....	11
7.	Experimental setup for SHG measurements .....	12
8.	Corona discharge assembly used for in situ monitoring of SHG signal .....	12
9.	Relative SHG intensity versus temperature change during poling process for sample No. 2 .....	15
10.	Absorption spectra of thin films .....	15
11.	Decay of second harmonic intensity at room temperature .....	16
12.	Decay of second harmonic intensity at 100°C .....	17

## **1. INTRODUCTION**

---

Over the past decade, fiber optic communication bandwidths in practical use have steadily increased from the MHz to the GHz range, in response to requirements from the telecommunications, computer network and cable TV industries. This trend is certain to continue, far outpacing current methods for impressing data onto laser signals by modulating laser sources directly, which has already met its practical limit ( $\approx 10$  GHz). Future improvements depend completely on the use of external waveguide modulators. Lithium niobate waveguide modulators are now commercially available with bandwidths up to ( $\approx 10$  GHz); however, this capability also will soon be exceeded as demand for data rates continues to grow. In the next decade, waveguide modulators with 50 GHz bandwidth will be required. Such devices will enable, for example, 500 channels of cable TV to be delivered to the home, widespread direct access to off-site supercomputers, and other infrastructure technologies to support growing Government and commercial needs.

These bandwidth requirements cannot be met by lithium niobate and other crystalline inorganic materials used in such modulators, for the basic physical reason that the relatively large dielectric constants of all such materials imply a strict high frequency limit on the order of 10 GHz - regardless of other electro-optic properties.

It is widely agreed that the most promising solution lies in organic and polymeric electro-optic (E-O) modulator materials, whose intrinsically low dielectric constants permits theoretical bandwidths up to 100 to 150 GHz, and whose processibility into films is adaptable to waveguide optics. We also note that development of such materials will be beneficial to other photonics applications such as high speed beam scanning using phase array elements and frequency doubling of low power diode lasers.

To date, however, a technical barrier that has emerged for implementing this solution is in finding a practical electro-optic polymer. In spite of efforts in many laboratories around the world and research on a variety of second order organic materials, no practical, processible waveguide material has emerged which combines four key properties:

- Large electro-optic coefficient ( $r$ ).
- High bandwidth.
- Low optical loss.
- Chemical and physical stability.

A major problem is the tradeoff which has been observed between a large electro-optic coefficient ( $r$ ), and its long-term stability (1-6). It is a common feature of polymer chemistry and processing that stability requires high temperature processing. Unfortunately, high temperature processing and poling tends to 1) limit the degree to which a polymer can be poled, and 2) decompose the chromophores responsible for large  $r$ , therefore decreasing the e-o coefficient.

As a result, polymers that do possess large electro-optic effects almost invariably are environmentally unstable, deteriorating after a few hours or days, and far too soft for

incorporation into devices (4). To date, performance and practicality in organic e-o films have not been found together in a single material.

### 1.1 Low Temperature Processing - Key to Stability

A key to solving this dilemma - and enabling practical, high bandwidth modulators for the technological communication needs of the next century - will be to identify and develop stable, strongly electro-optic films which can be processed at low temperatures. Methods to accomplish this are the focus of this report.

Electro-optic active elements incorporated in these polymers are dye-like chromophores that are added to form *guest-host* systems. Most commonly used electro-optic chromophores have a short lifetime at elevated temperatures. It is crucial, therefore, that the guest-host polymers be processible at room temperature or at slightly elevated temperatures. In compliance with this requirement, *the polymer that is the subject of this report can be doped and processed further at or below room temperature.* Avoiding high temperature processing, usually required for curing stable polymers reported to date, prevents the thermal destruction of these chromophores.

### 1.2 Summary of Phase I Research

To our best knowledge, the polymer shown in Figure 1, which has only become available in the past 12 months, has not been explored for these purposes before. In this program, we produced and characterized a new class of e-o polymer based on a polyarylate with the structure shown in Figure 1. The guest material was 4-morpholino-4'-nitrostilbene (MNS), (Figure 2) and was provided by Laser Photonics Technology, Inc.

The following sections provide background material on materials for second order nonlinear optical applications, experimental procedures and results, and the conclusions of the Phase I program.

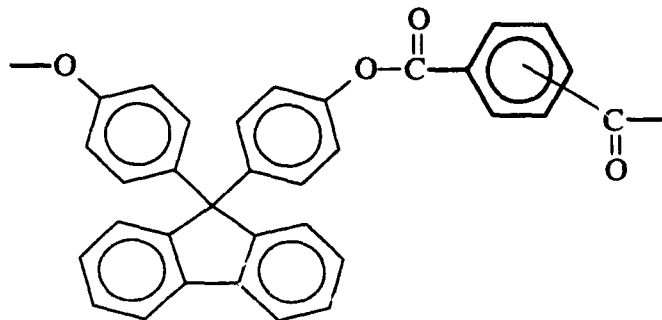


Figure 1. Structure of polyarylate

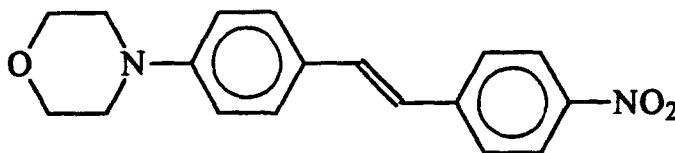


Figure 2. Structure of NLO chromophore, MNS

## 2. BACKGROUND

### 2.1 Electro-Optical and Second Harmonic Generation Waveguide Device Requirements

In order to construct high frequency integrated electro-optic modulators, a large number of optical materials and device orientations have been investigated. In this section we will compare the advantages and disadvantages of these materials from both theoretical and practical points of view. This discussion is based on the evaluation of a Mach-Zehnder Interferometer (Figure 3). However, the results are ultimately independent of other device configurations, such as directional couplers and TE-TM converters, since they are all based on modulation of the index of refraction in channel waveguides. In this section we compare three important Figures of Merit (FOM) for these materials (Table 1). These FOMs include: sensitivity ( $Q_1$ ) (defined as phase change per unit energy per unit voltage), frequency bandwidth ( $W$ ) and insertion loss. We will also compare the FOM for frequency doubling applications. Comparison of these figures of merit indicate very clearly the advantages of organic electro-optic polymers.

The Figure of Merit ( $Q_1$ ) measures the change in index ( $\Delta n$ ) per unit energy ( $w$ ) and per unit applied field ( $E$ ). Calculating  $Q_1$  for a stripline waveguide orientation such as that shown in Figure 3 gives:

$$\frac{\Delta n}{wE} \propto \frac{n^3 \Gamma}{\epsilon} = Q_1$$

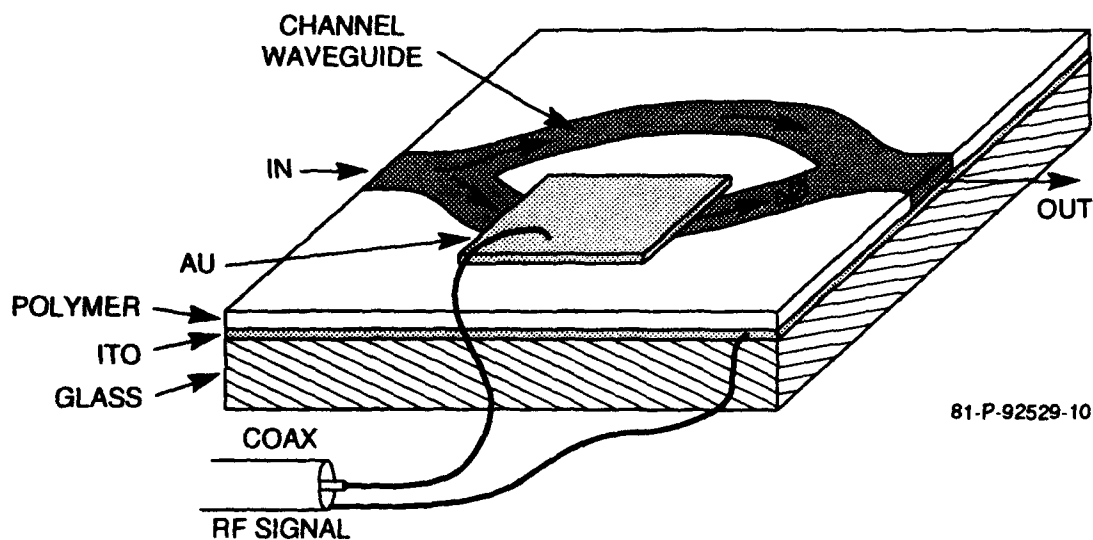


Figure 3. Mach-Zehnder interferometer

**Table 1. Figures of merit for electro-optic devices**

Material	$r$ (pm/V)	$\chi^{(2)}$ (pm/V)	Power Requirements (W/modulator)	Switching Voltage (V) (for a 1 mm thick device)	Polarization Lifetime	Fabrication Cost/Device	Temperature Range	Q1 Figure of Merit for EO Applications	Q2 Figure of Merit for SHG Applications	Bandwidth-Length Product $L_{max} \cdot f_m$ (GHz · cm)
								$(n^3/r/\epsilon_r)$ (pm/V)	$\chi^{(2)2}/n^3$ (pm/V) <sup>2</sup>	
LiNbO <sub>3</sub>	30	10	0.6-5	3.5-10.5	Unlimited	\$5,000(b)	<500°C	12	6.4	6, 30(a)
Present polymers [3]	20-100	10-150 [3]	0.2	1.3-2 [3]	Weeks-months	<\$5,000(b)	80-200°C	58	20-4500	150
Present polymers with Foster-Miller's new poling process	20-100	10-150	0.2	1.3-2	Years-decades	<\$5,000(b)	Up to and beyond 300°C	58	500-4500	>150
Target Value	>100	≥100	<0.1	1-5	20 years	<\$10(c)	150°C 20 years 300°C hr	>50	>2000	>150

(a) Using intermittent intraction electrodes.

(b) Price for laboratory level production.

(c) Mass production.

where  $\epsilon$  is the relative dielectric constant of the material. Almost all inorganic materials with large electro-optic coefficient  $r$  have also very large dielectric constants, for example  $\epsilon_{33} = 30$  in the case of  $\text{LiNbO}_3$ . This is almost 10 times larger than the dielectric constant of electro-optic polymers ( $\epsilon_{33} < 3$ ) that have comparable electro-optic coefficients with  $\text{LiNbO}_3$  (13). As a result of this large difference electro-optic polymers have significantly higher  $Q_1$  typically by a factor of five.

The most important FOM, sets an upper bound for device bandwidth. The significance of this FOM becomes clear when one considers the following problem: what is the shortest electrical pulse that can be converted to an optical pulse without distortion. In Figure 4, a microwave pulse of time width  $T$  (corresponding to a bandwidth  $f = 1/T$ ) will travel in the microwave transmission line with an effective dielectric constant of  $\epsilon_{\text{eff}}$ . It phase modulates the same section of the traveling optical beam without distortion if the optical velocity  $c/n$  is the same as the microwave velocity  $c/(\epsilon_{\text{eff}})^{1/2}$ . Any difference between these velocities determines how long the interaction length can be or how short the electrical pulse may be. The difference between these two velocities puts a limit on the bandwidth-length product  $W$  that we calculate to be:

$$W = fL < \frac{c}{n - \sqrt{\epsilon_{\text{eff}}}}$$

In  $\text{LiNbO}_3$ , the optical velocity is 2.5 times faster than the microwave frequency whereas in electro-optic polymers this factor is almost unity (1.05). The optical-microwave velocity mismatch is the single most important factor determining the superiority of electro-optic polymers over  $\text{LiNbO}_3$ . Owing to their small optical and microwave velocity mismatch, polymers can be used in waveguide optical modulators with modulation frequencies exceeding 150 GHz, compared to only about 6 GHz in  $\text{LiNbO}_3$ . With complicated intermittent interaction electrodes (IIE), modulation frequencies as high as 30 GHz in  $\text{LiNbO}_3$  are obtained.  $\text{LiNbO}_3$  devices with IIE, however, require much higher powers (10 times and higher) than polymer modulators (14). Furthermore, planar and channel waveguides of polymers can be fabricated at much lower costs than those in  $\text{LiNbO}_3$ . Specific expected values of relevant properties and tradeoffs were shown in Table 1.

Optical insertion loss is also an important determining factor and has two components: the fiber-coupling loss and the through-chip waveguide loss. Typically, the sum of these losses in  $\text{LiNbO}_3$  is about 4 dB with only 0.5 db/cm contribution due to the waveguide absorption loss. In polymeric waveguides however this insertion loss is larger approximately 4 to 10 dB (15). Reduction of insertion loss is one of the important factors in designing new polymeric materials

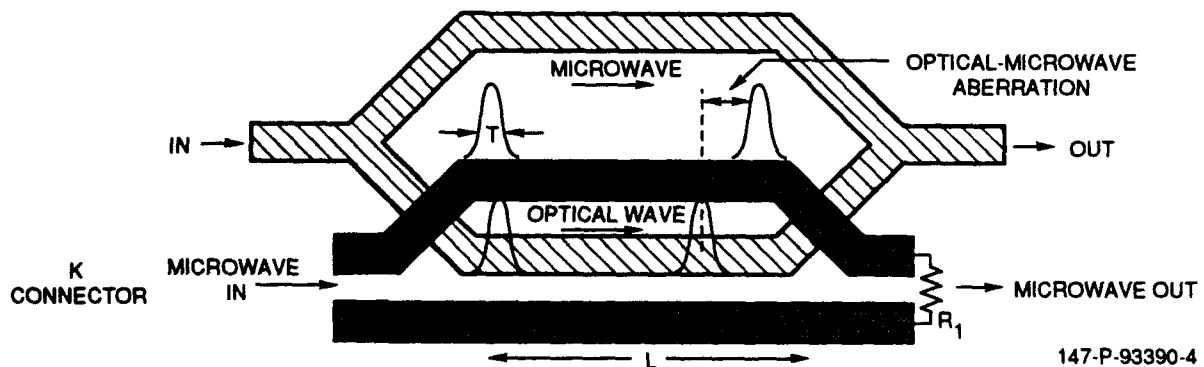


**Figure 4. The difference between the optical and microwave velocities limits the ultimate bandwidth of a traveling wave modulator**

as well as coupling methods that could significantly reduce the total loss. Other important parameters, also discussed in Table 1 are power and voltage requirements. As a consequence of a larger nonlinear sensitivity  $Q_1$ , electro-optic polymers require lower voltages and switching powers. In particular, power dissipation is of significant importance since it ultimately determines the price per serving channel of cable TV. It also determines the lifetime of a device since most of the power will be dissipated thermally affecting the long-term chemical composition of not only the polymeric materials but also that of  $\text{LiNbO}_3$ .

#### *Figure of Merit for Frequency Doubling*

SHG in waveguides is of great interest for applications using low power lasers. In a waveguide, the second harmonic generated signal intensity is given by:

$$I_{2\omega} = (k_0 L)^2 |K|^2 [\chi_{\text{eff}}^{(2)2} / 4 N^{3(m, \omega)}]$$

$$[\sin(\Delta k L) / \Delta k L]^2 I_{\omega}^2$$

where,

$$\Delta k = 2 [N^{(m, 2\omega)} - N^{(m, \omega)}] k_0,$$

$N^{(m, \omega)}$  is the waveguide index of mode number  $m$  and frequency  $\omega$ ,  $\chi^{(2)}$  is the effective Chi-2 coefficient of the material,  $k_0$  is the optical wavevector,  $\Delta k$  is the phase mismatch,  $L$  is the interaction length and  $K$  is an overlap integral describing the effective overlap of the fundamental (in mode  $m$ ) and the second harmonic field (in mode  $m$ ). The figure of merit in this case is:

$$Q_2 = \chi_{\text{eff}}^{(2)2} / N^{3(m, \omega)}$$

In contrast to the FOM for the electro-optical devices ( $Q_1$ ),  $Q_2$  is inversely proportional to the index (cube of index). The contribution due to this difference is however at most a factor of 2 to 3.

## **2.2 Novel, Room Temperature Processible, Stable Electro-Optic Polymers**

Despite clear advantages of polymeric materials over inorganic materials, a number of basic problems are yet to be resolved before polymers can be used in practical applications. The number one problem is the thermal stability and its effects on polarization retention time of polymers. Recently many polymers with long polarization lifetimes have been reported. Among these polymers, dye doped polyimides reported by the Lockheed (4-6) and the IBM groups (7) have exhibited the most stable material reported to date with only a few percent reduction of their E-O coefficient over 300 hr at 200°C. These standard polyimides however require long, high temperatures (~300°C) curing cycles. At these temperatures, most commonly used NLO chromophores such as the disperse red-1 disintegrate resulting in small electro-optic coefficients after poling. Finally, most high  $T_g$  electro-optic matrix polymers are highly absorbing the visible and near IR causing high insertion loss and low quantum efficiency.

In order to identify suitable polymers with high enough  $T_g$ , solubility and transparency we have conducted an extensive search covering a large number of polyarylates and polyimides. Polyarylates and aromatic polyimides are generally known for their high glass transition temperatures ( $T_g$ ) and low solubility in common organic solvents. Extensive research in both systems has been carried out to discern the effect of structure on solubility and  $T_g$ . This has recently been achieved by introducing "kinks" and sterically bulky separator groups into the

polymer backbone between the aromatic ester units. The introduction of these structures increases chain flexibility and interchain spacing resulting in increased solubility without significant reductions in  $T_g$ . In addition this reduces formation of interchain charge transfer complexes (CTC) that usually give rise to broad absorption in the visible wavelength range. The key to achieving this effect is increasing the distance between adjacent polymer chains while maintaining an approximately linear polymer backbone with some limited flexibility.

This strategy has recently resulted in the development of new polyarylates such as polyarylate x15 and polyarylate x25, with enhanced solubility while retaining a high  $T_g$ . In these polymers, ester linkages connect very large aromatic monomers. The resulting chains are kinked, with low chain-to-chain interaction, permitting *high solubility, negligible visible and infrared absorption and high  $T_g$* . These polymers, first developed by Isonova Inc. have  $T_g$ s on the order of 250 and 350°C respectively. Other soluble polyarylates with high  $T_g$  can be produced by selecting appropriate structural variations.

These general trends for polyarylates can be extended to the aromatic polyimides. Introducing sterically bulky separator groups and *kinks into the polymer backbone will also result in the reduction of color*. Standard aromatic polyimides are generally colored due to the formation of interchain CTC. Sterically bulky separator groups and kinks will increase the distance between adjacent polymer chains decreasing the tendency for CTC formation. Selection of separator groups with appropriate electronegativities can further reduce color by decreasing the magnitude of CTC if formed. Aromatic polyimides with increased solubility, decreased color and high  $T_g$  have been produced by employing these techniques. For applications as electro-optic polymers, we have identified two such polyimides IPAN-4,4'-6F and Triphenylphosphineoxide - Phenylene Diamine that are colorless, are soluble and have  $T_g$ s of 304°C and 300°C respectively.

The Phase I effort concentrated on fabricating and testing a guest-host electro-optic polymer based on a polyarylate.

### 2.3 Principle of Poling Induced Second-Order Nonlinearity in NLO Films

The most widely used means to achieve noncentrosymmetry in a side-chain polymer or dopant/polymer material is the technique of electric field poling. The effectiveness of the poling process depends on a variety of factors such as the temperature, strength and duration of the poling electric field, the ambient environment, the material itself and how it may have been cured. In order to determine the optimal poling conditions, the in situ poling technique is often applied, in which the second-harmonic intensity or the electrooptic modulation signal is monitored while different poling parameters are varied.

The poling process induces a polar axis in the material which is essentially an infinite fold rotational axis with an infinite number of mirror planes. According to the Kleinman's symmetry argument and thermodynamic considerations, there are only two nonvanishing elements of the second-order susceptibility tensor, namely,  $\chi_{zzz}^{(2)}$  and  $\chi_{zxx}^{(2)}$ , which are related to the molecular hyperpolarizability,  $\beta$ , the dipole moment,  $\mu$ , and the poling electric field, E, by:

$$\chi_{zzz}^{(2)}(\omega_3; \omega_1, \omega_2) = \frac{fN\mu\beta E_p}{5kT} \cdot \chi_{zxx}^{(2)}(\omega_3; \omega_1, \omega_2) = \frac{1}{3}\chi_{zzz}^{(2)}(\omega_3; \omega_1, \omega_2) \quad (1)$$

where  $kT$  is the Boltzman thermal energy.

For electric field poled polymeric thin films coated on glass substrates, the second-harmonic light intensity can be expressed by:

$$I_{2\omega} = \frac{512\pi^3}{A} t_{\omega}^4 T_{2\omega} t_o^2 d^2 p^2 I_{\omega}^2 \frac{\sin^2 \psi(\theta)}{(n_{2\omega}^2 - n_{\omega}^2)^2} \quad (2)$$

where  $I_{\omega}$  is the fundamental laser power,  $A$  is the area of the laser beam spot,  $d = \chi^{(2)}/2$  is the appropriate second-harmonic coefficient in the contracted notation,  $p$  is the angular factor which projects the nonlinear susceptibility tensor onto the coordinate frame defined by the propagating electric field, and the  $n$ 's are the refractive indices at the appropriate frequencies. The transmission factors  $t_o$  and  $T_{2\omega}$  are given by:

$$t_o = \frac{2n_o \cos \theta_o}{\cos \theta_o + n_o \cos \theta}$$

$$T_{2\omega} = 2n_{2\omega} \cos \theta_{2\omega} \frac{(n_{\omega} \cos \theta_{\omega} + \cos \theta_{\omega})(n_{2\omega} \cos \theta_{\omega} + n_{\omega} \cos \theta_{2\omega})}{(n_{2\omega} \cos \theta_{2\omega} + \cos \theta)(n_{2\omega} \cos \theta_{2\omega} + n_o \cos \theta_o)^2} \quad (3)$$

where  $\theta$  is the angle of incidence,  $\theta_{\omega}$  and  $\theta_{2\omega}$  are the internal angles of the fundamental and the second-harmonic beams, respectively, and  $\theta_o$  is the internal angle of the second-harmonic beam inside the substrate. The factor  $p$  and the transmission factor  $t_{\omega}$  depend on the polarization of the fundamental and harmonic light beams. When the fundamental laser beam and the transmitted second-harmonic are both p-polarized and with the assumption of  $d = d_{33} = 3d_{31}$ , then

$$t_{\omega} = \frac{2 \cos \theta}{n_{\omega} \cos \theta + \cos \theta_{\omega}}$$

$$p = \left( \frac{1}{3} \cos^2 \theta_{\omega} + \sin^2 \theta_{\omega} \right) \sin \theta_{2\omega} + \frac{2}{3} \cos \theta_{\omega} \sin \theta_{\omega} \cos \theta_{2\omega} \quad (4)$$

and when the incidence laser beam is s-polarized and the second-harmonic light p-polarized and with  $d = d_{31}$ ,

$$t_{\omega} = \frac{2 \cos \theta}{n_{\omega} \cos \theta_{\omega} + \cos \theta}$$

$$p = 2 \sin \theta_{\omega} \cos \theta_{\omega} \cos \theta_{2\omega} \quad (5)$$

The angular dependence term,  $d = d_{31}$ , of the second-harmonic intensity, can be expressed as:

$$\psi(\theta) = (\pi L / 2) (4 / \lambda) (n_{\omega} \cos \theta_{\omega} - n_{2\omega} \cos \theta_{2\omega}) = \pi L / 2 \ell_c \quad (6)$$

where  $\ell_c = \lambda / 4(n_{\omega} \cos \theta_{\omega} - n_{2\omega} \cos \theta_{2\omega})$  is the coherence length. At normal incidence,  $\ell_c = \lambda / 4(n_{\omega} - n_{2\omega})$ .

It is apparent that when the film is rotated around an axis perpendicular to the laser beam, the second-harmonic intensity changes as a function of the rotation angle. The angular dependent second-harmonic curve is called the Maker fringes. Since the film thickness is usually much smaller than the coherence length (typically around  $20 \mu\text{m}$ ), only the envelope of the Maker fringes is observed. Typical SHG curves from a  $1 \mu\text{m}$  thick poled film with different polarization combinations are presented in Figure 5.

The second-order susceptibility of a poled material is evaluated by comparing the second-harmonic intensity generated from the material to that from a Y-cut quartz crystal which has a  $d_{11}$  value of  $1.2 \times 10^{-9}$  esu. Material in the form of thin films are mounted on a rotation stage and rotated perpendicularly to the laser beam. The obtained angular dependence curves are computer fitted and the maximum intensity is compared to the envelope of the Maker fringes from the quartz crystal.

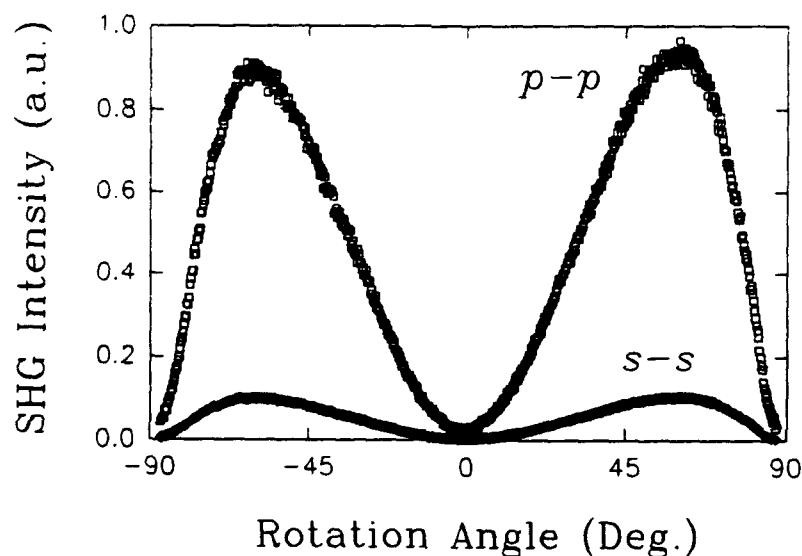


**Figure 5. Angular dependence of the SHG intensity from an electric field poled thin film for different polarization combinations**

### 3. EXPERIMENTAL PROCEDURES

---

#### 3.1 Materials and Sample Preparation

Our approach in designing effective and stable second order NLO guest host material consisted of synthesizing a chromophore with large  $\beta$  value and dispersing it in a high Tg polymer matrix. The NLO chromophore, 4-morpholino-4'-nitrostilbene, MNS (see Figure 2 for chemical structure) was synthesized in a Wittig reaction of N,N-(diethoxyacetyl)amino-benzaldehyde with 4-nitrobenzyltriphenylphosphonium bromide in an ethanol solution of sodium ethoxide. The reaction was carried out over 10 hr at 60°C; the product was separated by filtering the reaction mixture quenched with cold water and purified by column chromatography giving a yield of 30 percent. Figure 6 shows mass spectroscopy and NMR spectra of MNS characteristic of high purity chromophore. Differential scanning calorimetry was used to establish the thermal stability of the compound. The results showed that MNS molecule is thermally stable up to 260°C. Molecular second order optical nonlinearities of MNS were not measured.

However, based on first hyperpolarizability ( $450 \times 10^{-30}$  esu) and dipole moment (7.4 D) values of 4-N,N-dimethylamino-4'-nitrostilbene (DANS) (J.L. Oudar, J. Chem. Phys., 67, 446, 1977) the nonlinearity of MNS was expected to be large.

Solutions of Isaryl-25 (high Tg polyester) in N-methyl pyrrolidone (NMP) containing 15 weight percent of MNS were used to prepare film samples. Thin films of the composite material were deposited on ITO coated glass substrates by spin casting technique. The films were initially dried at room temperature for several hours in order to remove excess solvent and, subsequently, placed in an electric field poling apparatus (described below) for second harmonic generation (SHG) investigations.

#### 3.2 Setup for SHG Measurements

The experimental setup for second harmonic generation is schematically shown in Figure 7 and is comprised of the following main components:

1. A Q-switched pulsed Nd:YAG laser providing a 1.06  $\mu\text{m}$  fundamental beam with a pulse width of  $\sim 10$  ns and repetition rate of 10 Hz.
2. A nonlinear optical (NLO) film sample to which a dc-field could be applied; the 1.06  $\mu\text{m}$  fundamental radiation is directed on the sample at an incident angle of 45 to 55 deg.
3. A photomultiplier tube (PMT) as a detector of the SH signal generated by the NLO film; a set of IR (1.064  $\mu\text{m}$ ) cut-off and narrow band-pass (532 nm) interference filters is placed at the PMT's entrance slit to remove the fundamental and other background radiation from the SHG signal.

The dc-field was applied to the NLO film sample using a corona discharge device as shown in Figure 8. It consists of a metal stage with built-in resistive heaters. A thermocouple and a programmable power supply are used to control and ramp the temperature over a 25 to 350°C

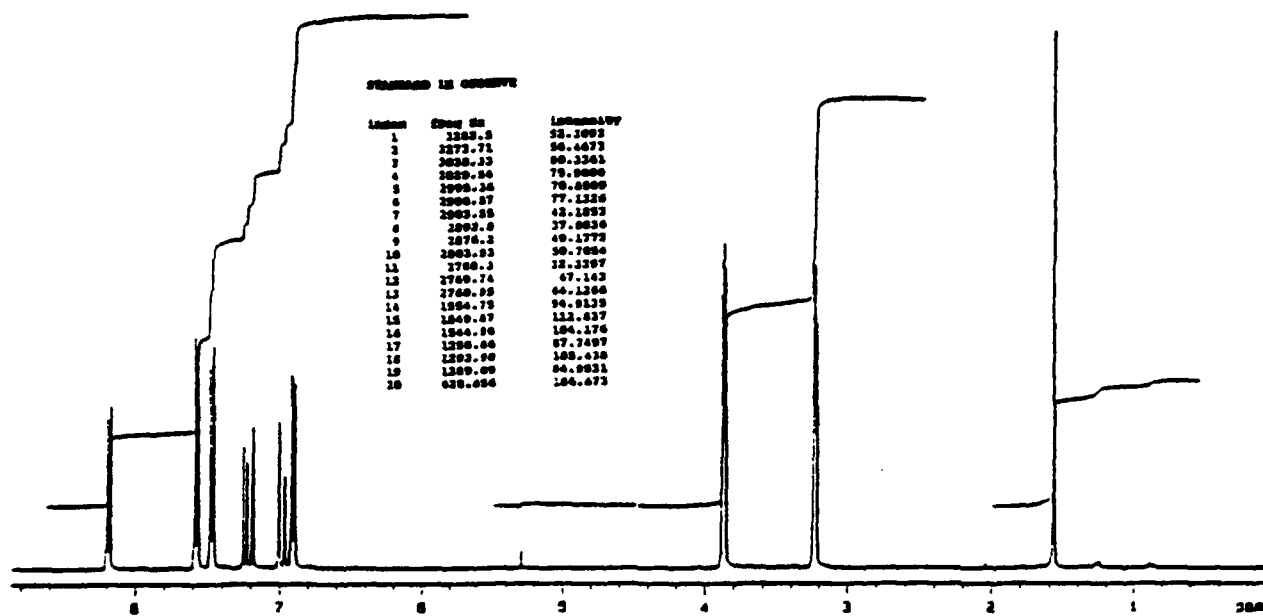
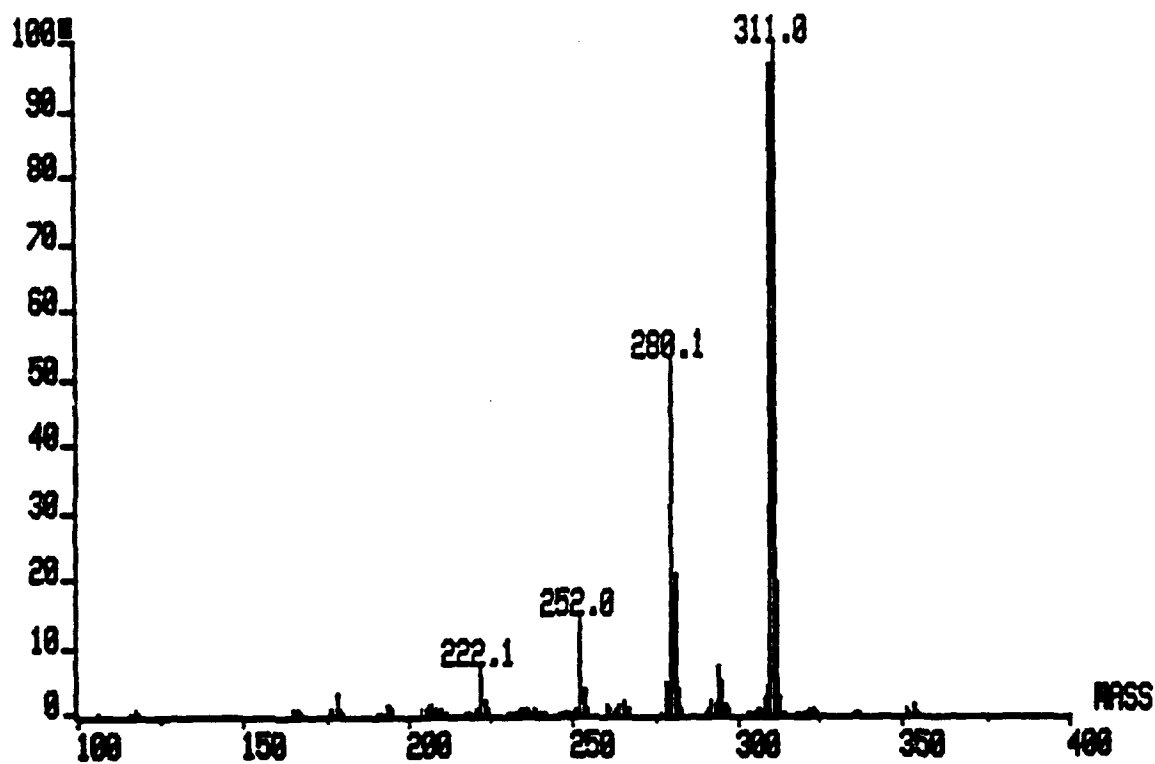
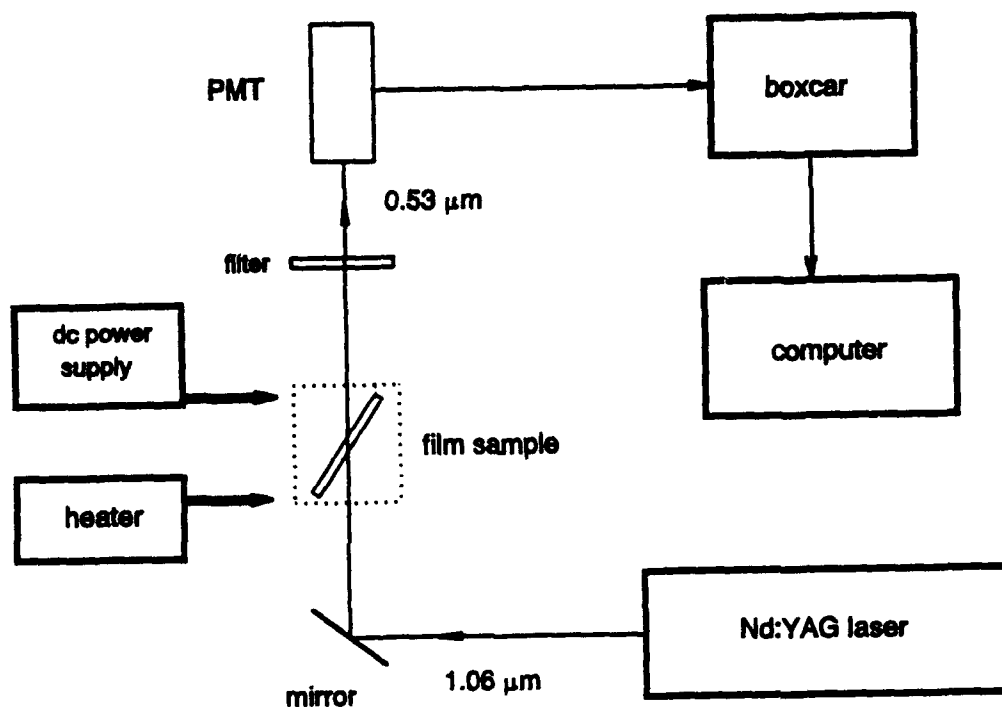
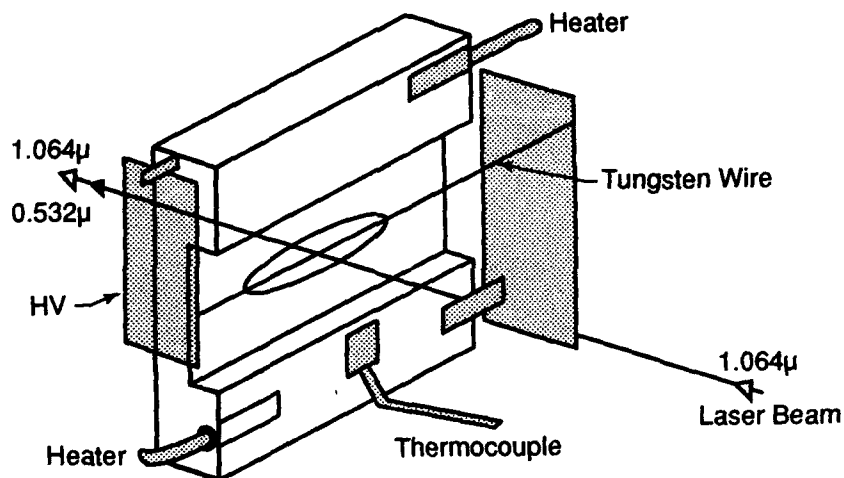


Figure 6. Mass spectroscopy (upper trace) and  $^1\text{H-NMR}$  (bottom trace) spectra of MNS chromophore



**Figure 7. Experimental setup for SHG measurements**



259-AFB-09740-1

**Figure 8. Corona discharge assembly used for in situ monitoring of SHG signal**

temperature range. The polymer film sample is mounted on the stage with an electric contact being made between ITO layer and the stage. A 25 μm thick tungsten wire is placed about 10 mm above the film surface and used as the positive electrode while the ITO layer functions as the negative (or ground) electrode. A corona discharge was generated in the air by applying a high voltage (4.5 to 5 kV) to the tungsten wire.

## 4. RESULTS AND DISCUSSION

---

### 4.1 Poling Characteristics of Tested Film Samples

The electric field poling efficiency depends on a large number of parameters such as the poling temperature, poling electric field, ramp schedule, environmental humidity and the material curing processes. The optimal poling conditions vary from one material to another. In order to perform more efficient electric field poling, one has to determine the best poling conditions for each material. We have conducted in situ poling second-harmonic generation studies on the polymeric composites by monitoring the SHG intensity from the material while different poling parameters are varied either individually or simultaneously. A p-polarized fundamental beam was used for all the second-harmonic generation in situ measurements.

In this section we briefly describe the measured SHG behavior of a number of film samples made from the same NLO material under different conditions of corona discharge configuration shown in Figure 8. Nine samples were tested at different poling conditions (poling voltage, heating temperature, and poling time). The key poling parameters are summarized in Table 2. In all the experiments, the overall poling process consisted of three stages:

1. Heating the sample from room temperature to the highest poling temperature ( $T_{\max}$ ) at a rate of  $5^{\circ}\text{C}/\text{min}$ .
2. Keeping the sample at  $T_{\max}$  for a time period of 10 to 45 min.
3. Cooling down the sample from  $T_{\max}$  to room temperature at a rate of  $5^{\circ}\text{C}/\text{min}$ .

The corona discharge field was kept on throughout the entire heating-cooling cycle. At the end of the poling process, the corona discharge field was turned off and the second-order nonlinearity of the poled samples were investigated by monitoring the temporal stability of SHG signal at different temperatures.

The data presented in Table 2 indicate that all samples could be effectively poled at room temperature. However, temporal stability of the induced alignment was very poor (maximum relaxation time of about 10 min) which is indicative of a large free volume within the polymer matrix. The high temperature poling process produced more stable alignment of the chromophores with varying temporal stability which depended upon the processing conditions. As an example, Figure 9 shows the relative SHG signal intensity as a function of temperature during the electric field poling procedure for sample No. 2. The poling time at  $T_{\max} = 250^{\circ}\text{C}$  was about 30 min. The hollow triangles are the data obtained during the heating-up process, and the hollow circles show the data from the cooling-down process.

The effect of poling temperatures was investigated with the use of UV-Vis spectroscopy. Figure 10 shows absorption spectra from three film samples that have the same thickness; curve (a) is obtained from an unpoled film, curve (b) from sample No. 9 poled at  $200^{\circ}\text{C}$ , and curve (c) from sample No. 8 poled at  $280^{\circ}\text{C}$ . One can clearly notice the reduction of the net absorption and the blue shift of the absorption peak as a result of the electric field poling and thermal treatments. In case of curve (b) the first effect is dominant which is solely due to

**Table 2. Poling characteristics of film samples**

Sample No.	Thickness of Film ( $\mu\text{m}$ )	Corona Voltage (kV)	SHG Intensity at 24°C (before heating) (mV)	Maximum Temperature $T_{\text{max}}$ (°C)	Time at $T_{\text{max}}$ (min)	SHG at $T_{\text{max}}$ (mV)	SHG at 24°C (after heating) (field on) (mV)	SHG at 24°C (after heating) (field off) (mV)	Effective $\chi^{(2)}$ (107 esu)
1	7.5	5		250	10	65	40	35	0.09
2	6.0	5	280	250	30	210	200	85	0.13
3	7.8	5	38	275	20	180	190	43	0.10
4	4.5	4	70	300	30	270	240	100	0.26
5	8.8	4	30	350~360	30	20	30	29	0.07
6	8.7	5		315	45	40	40	29	0.07
7	3.7	5	55	315	45	55	50 (@ 100°C)	40 (@ 100°C)	0.20
8	0.6	5	125	280	15	120	95	50	1.40
9	0.6	5	130	200	15	270	135	80	1.80

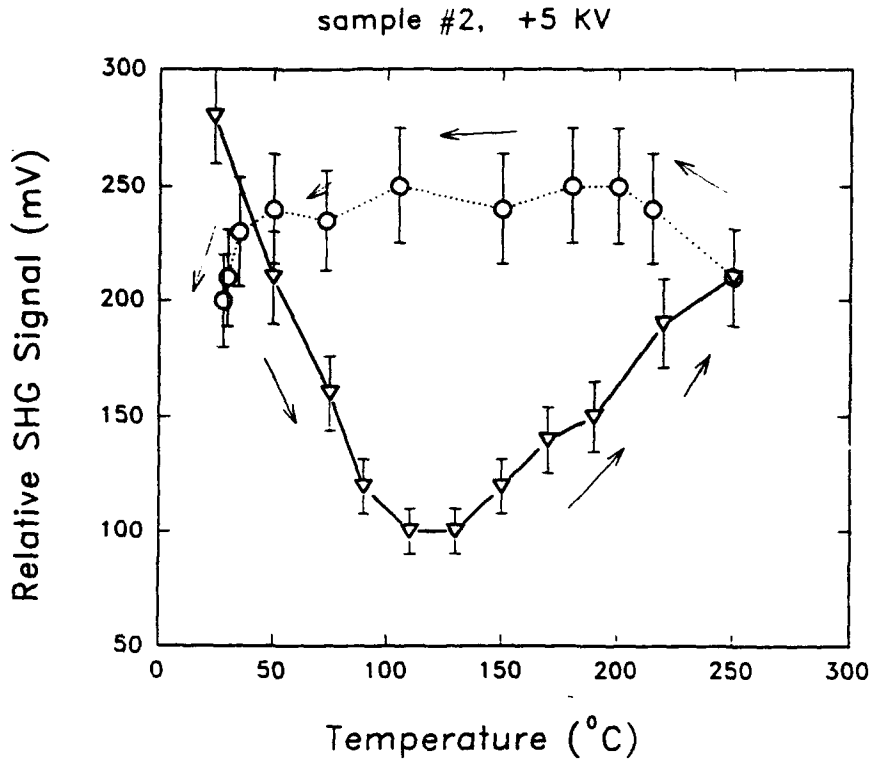


**Figure 9. Relative SHG intensity versus temperature change during poling process for sample No. 2**

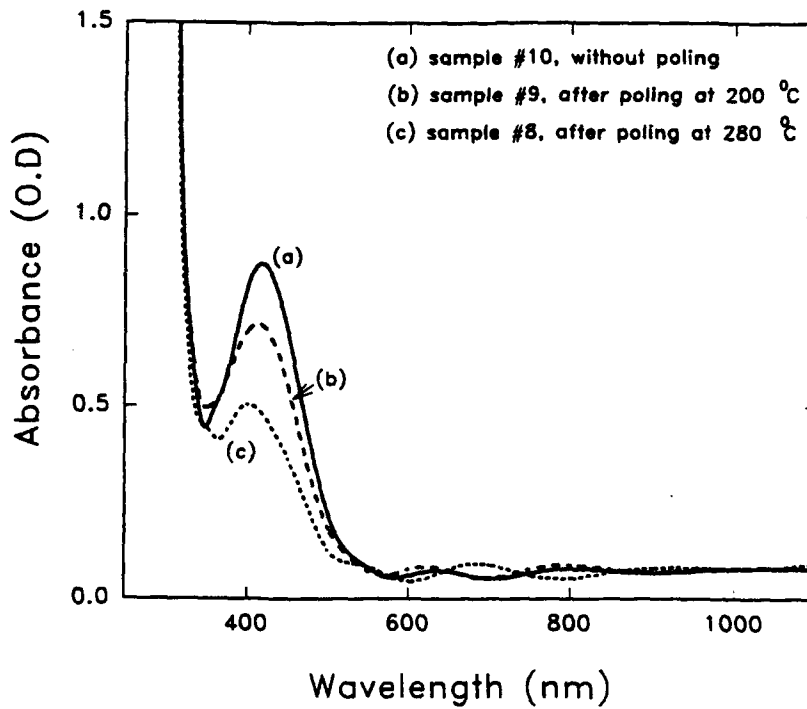


**Figure 10. Absorption spectra of thin films**

semipermanent electric field induced reorientation of the chromophore molecules at elevated temperatures. However, in case of curve (c) there is an obvious blue-shift of the peak position in addition to the reduction of absorption. The latter observation indicates that at poling temperatures above 260°C the chromophore molecules may either partially decompose or isomerize. Thermal decomposition involving break-up of the C=C double bond structure is very probable which should result in a disruption of the  $\pi$ -electron conjugation and, thus, dramatic change in the chromophore's electronic spectrum. For this reason, most of the samples were poled at temperatures which did not exceed 250°C.

#### 4.2 SHG Decay Behavior of Poled Film Samples

##### *Temporal Stability*

The in situ SHG experiments were conducted on several composite films containing the MNS chromophore. The in situ technique provides real-time information about the matrix and its ability to retain the chromophores in their preferred orientation. This property can change dramatically as the materials are thermally processed. The second-order chromophores were shown to be electrically aligned at room temperature. The decay of the second-harmonic signal was monitored as a function of heat treatment as summarized in Figure 11.

For sample No. 6 (poled at  $T_{\max} = 315^\circ\text{C}$  for 45 min) the SHG intensity was about 59 percent of the initial (as poled) value after 11 days. For sample No. 2 (poled at  $T_{\max} = 250^\circ\text{C}$  for 30 min) the SHG intensity was about 41 percent of the initial value after 26 days.

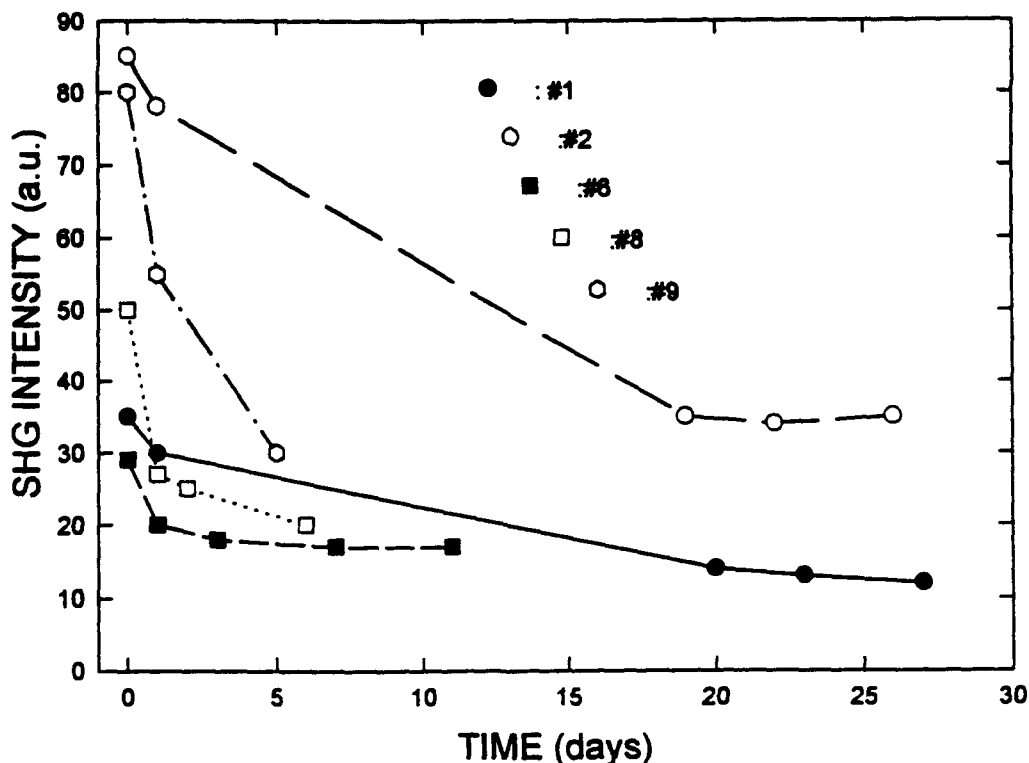


**Figure 11. Decay of second harmonic intensity at room temperature**

### Thermal Stability

Figure 12 summarizes the SHG decay behavior for four poled samples kept at 100°C. Keeping poled samples at elevated temperatures usually leads to a faster randomization (decay) of the induced noncentrosymmetric alignment because of a greater contribution from thermal relaxation (greater Boltzman energy). The best result was recorded for sample No. 7 that was poled at  $T_{\max} = 315^\circ\text{C}$  for 45 min. After 11 days of keeping this sample at 100°C, the SHG intensity was about 20 percent of the initial value.

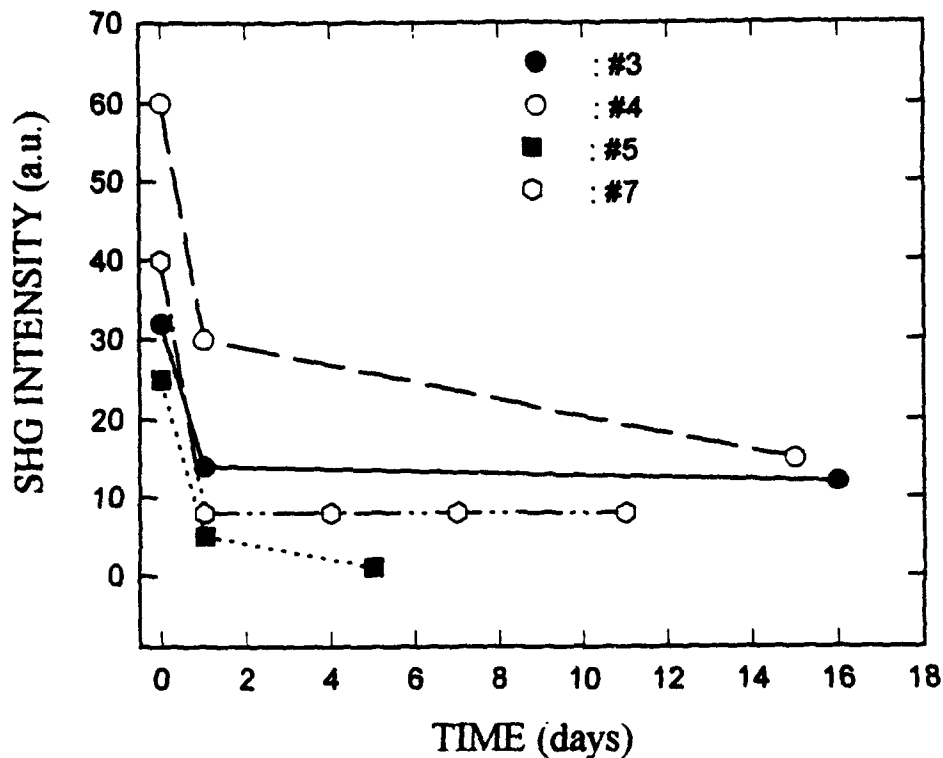


Figure 12. Decay of second harmonic intensity at 100°C

## 5. CONCLUSIONS

---

There are several requirements imposed on a  $\chi^{(2)}$  material; four of them are imperative if it is to be effective in a real device. These are:

1. Large  $\chi^{(2)}$  value.
2. Optical transparency.
3. Ease of processing into a desired form.
4. Temporal and thermal stability of the second order responses.

The strength of the second order response, the ability of the matrix to retain the noncentrosymmetric alignment and the results illustrating the low losses obtained from wave guides are all necessary achievements if these materials are to be used in commercial integrated electro-optical devices.

There are several organic materials that are being developed in a large number of research groups; these efforts are driven by the fact that organic materials have high optical nonlinearities and can be more readily processed. Polymers as a whole have had the reputation of not being sufficiently rigid to retain noncentrosymmetric alignment. In other words, they could be poled, but were found to readily relax. The use of polyimides, main chain polymers, and cross-linkable polymers have given these materials new promise. The materials discussed in this report meet many of the above requirements for effective second order NLO materials: they are tractable and exhibit large and  $\chi^{(2)}$  values. However, continued efforts should be directed at:

1. Improvement on the thermal stability of the non-centrosymmetric alignment of the chromophores.
2. Assessing the full potential of these materials for commercial applications.

For any real device, one may expect that the environmental conditions (e.g., temperature) may not necessarily be kept constant over a long period of time or during the device fabrication process. Thus, a major concern, to be more fully addressed, is whether these materials will maintain the alignment of the dispersed chromophores at elevated temperatures over an extended time period (months).

## 6. REFERENCES

---

1. W. Wu., J.F. Valley, S. Ermer, E.S. Binkley, J.T. Kenney, G.F. Lipscomb, and R. Lytel, *Appl. Phys. Lett.* **58** (1991) 226; J. W. Wu., E.S. Binkley.
2. D. G. Griton et al., *Appl. Phys. Lett.* **58** (16) (1991), 1730.
3. J. W. Wu. et al., *Appl. Phys. Lett.* **59** (18) (1991), 2214.
4. Y. M. Chen, "Optical and Electrical Properties of Polymers," Materials Research Society Symposium Proceeding, 1990, Boston, Volume 214, p. 35.
5. B. Dick, R.M. Hochstrasser and H.P. Trommsdorff, chapter in *Nonlinear Optical Properties of Organic Molecules and Crystals*, Vol. 2. Edited by D. S. Chemla and J. Zyss, 1987, Academic Press New York.
6. M. Stahelin, et al., *Appl. Phys. Lett.* **61**(11) (1992), 1627.
7. M.A. Druy an P.J. Glatkowski, "Nonlinear Optics" SPIE Symposium Proceedings Volume 1409, (1991).
8. Anne K. St. Clair et al., to appear in SPE ANTEC 1993 Conference proceedings, May 9-13, 1993 New Orleans, LA.
9. James McGrath, Private communications.
10. M.A. Druy, P.J. Glatkowski, and R. Burzynski, "Electrical, Optical, and Magnetic Properties of Organic Solid-State Materials," Materials Research Society Symposium Proceedings, 1991, Boston, to be published.
11. J. Swiatekiewicz, P.N. Prasad, F.E. Karasz, M.A. Druy, and P.J. Glatkowski, *Appl. Phys. Lett.* **56**, (1990) 892.
12. P. Tayebati, R. Kovar, L. Domash, "Development of New Organic Photo-refractive Nonlinear Optical Materials," Final report for Naval Surface Warfare Center, July, 1991.
13. Mai Chen et al., *American Chemical Society* 24(19), p.5421, 1991.
14. Schaffner, J.H. and R.R. Hayes, *Integrated Photonics Research*, 1991.
15. C. C. Teng, *Appl. Phys. Lett.* **60**, (1992) 1538.